

J-BAND INFRARED SPECTROSCOPY OF A SAMPLE OF BROWN DWARFS USING NIRSPEC ON KECK II ¹

Ian S. McLean²,

Mavourneen K. Wilcox², E. E. Becklin², Donald F. Figer³, Andrea M. Gilbert⁴, James R. Graham⁴, James E. Larkin², N. A. Levenson⁵, Harry I. Teplitz^{6,7}, J. Davy Kirkpatrick⁸.

ABSTRACT

Near-infrared spectroscopic observations of a sample of very cool, low-mass objects are presented with higher spectral resolution than in any previous studies. Six of the objects are L-dwarfs, ranging in spectral class from L2 to L8/9, and the seventh is a methane or T-dwarf. These new observations were obtained during commissioning of NIRSPEC, the first high-resolution near-infrared cryogenic spectrograph for the Keck II 10-meter telescope on Mauna Kea, Hawaii. Spectra with a resolving power $R \approx 2500$ from 1.135 to 1.360 μm (approximately J-band) are presented for each source. At this resolution, a rich spectral structure is revealed, much of which is due to blending of unresolved molecular transitions. Strong lines due to neutral potassium (K

¹ Data presented herein were obtained at the W.M. Keck Observatory, which is operated as a scientific partnership among the California Institute of Technology, the University of California and the National Aeronautics and Space Administration. The Observatory was made possible by the generous financial support of the W.M. Keck Foundation.

²Department of Physics and Astronomy, University of California, Los Angeles, CA, 90095-1562

³Space Telescope Science Institute, 3700 San Martin Dr., Baltimore, MD 21218

⁴ Department of Astronomy, University of California, Berkeley, 601 Campbell Hall, Berkeley, CA, 94720-3411

⁵ Johns Hopkins University, Department of Physics and Astronomy, Baltimore, MD 21218

⁶Laboratory for Astronomy and Solar Physics, Code 681, Goddard Space Flight Center, Greenbelt MD 20771

⁷NOAO Research Associate

⁸Infrared Processing and Analysis Center, M/S 100-22, California Institute of Technology, Pasadena, CA 91125

I), and bands due to iron hydride (FeH) and steam (H₂O) change significantly throughout the L sequence. Iron hydride disappears between L5 and L8, the steam bands deepen and the K I lines gradually become weaker but wider due to pressure broadening. An unidentified feature occurs at 1.22 μm which has a temperature dependence like FeH but has no counterpart in the available FeH opacity data. Because these objects are 3-6 magnitudes brighter in the near-infrared compared to the I-band, spectral classification is efficient. One of the objects studied (2MASSW J1523+3014) is the coolest L-dwarf discovered so far by the 2-Micron All-Sky Survey (2MASS), but its spectrum is still significantly different from the methane-dominated objects such as Gl229B or SDSS 1624+0029.

Subject headings: infrared: stars - stars: atmospheres - stars: low-mass, brown dwarfs

1. Introduction

After eluding undisputed detection for many years, numerous brown dwarfs – objects with sub-stellar mass – are now known. While some candidates were discovered in small-scale surveys of young nearby clusters, such as the Pleiades and Hyades, or as companions to low-mass stars, the biggest breakthrough has come as a result of large-scale surveys such as the Deep Near-Infrared Sky (DENIS) survey (Delfosse et al. 1997), 2MASS, the 2-Micron All-Sky Survey (Skrutskie et al. 1997, Kirkpatrick et al. 1999) and the Sloan Digital Sky Survey (SDSS) (Strauss et al. 1999). Recently, using optical (CCD) spectroscopy, Kirkpatrick et al. (1999) have defined a new spectral class, L-dwarfs, in which the metallic oxides (such as TiO and VO) found in M stars lose their dominance to metallic hydrides (such as FeH and CrH). The temperature range for the L class is given by Kirkpatrick et al. (2000) from about 2000 K for L0 to about 1250 K for L8, whereas Martin et al. (1999) suggest a range from 2200-1600 K. Depending on age and model calculations, Kirkpatrick et al. (1999) argue that at least one third of the L-dwarf objects must be brown dwarfs and perhaps all are.

Spectral classification is based on spectroscopy between 6500 and 10000 \AA at a resolution of 9 \AA ($R \sim 1000$). While use of this spectral region provides many important spectral diagnostics, it suffers from the fact that L- and T-dwarfs are extremely faint at these wavelengths and therefore long exposures on very large aperture telescopes are required to obtain spectra with good signal-to-noise ratios. Typical I-band magnitudes are

about 19 or fainter (*e.g.* GD165B), but a gain of 3-6 magnitudes can be obtained in going to the near infrared.

Using earlier generations of infrared instruments, previous observations of individual brown dwarf candidates have yielded a typical resolving power of about $R=500-1000$; see the observations of Geballe et al. (1996), Ruiz, Leggett and Allard (1997), Tinney, Delfosse and Forveille (1997), Kirkpatrick et al. (1999) and Strauss et al. (1999). These pioneering efforts were accomplished with instruments using an earlier generation of IR detector arrays, with at most 256×256 pixels. This resolution is sufficient to reveal the major differences that set apart the L-dwarfs and T-dwarfs from warmer stars, *e.g.*, the presence of deep steam bands and strong methane bands in the L- and T-dwarfs respectively. Kirkpatrick et al. (1993) modeled a spectral sequence of M-dwarfs using spectroscopy from 0.6 - 1.5 microns and identified the major bands and atomic features. Jones et al. (1996) performed a similar analysis from 1.16 - 1.22 microns with a sample of M dwarfs which also included GD165B. An excellent review of model atmospheres of very low mass stars and brown dwarfs is given by Allard et al. (1997).

In this paper we report observations using NIRSPEC, a new cryogenic infrared spectrograph on the Keck II telescope employing a 1024×1024 InSb array. A consistent set of J-band spectra with $R \sim 2500$ is presented which, for the first time, allows a detailed comparison of the near-infrared features of the spectral sequence from early L-dwarfs to T-dwarfs. Our targets were selected from the list of L-dwarfs published by Kirkpatrick et al. (1999) and supplemented with new sources discovered more recently by the 2MASS (Kirkpatrick et al. , 2000). One of these objects is reported as being the closest known L-dwarf to date and another is likely the coolest L-dwarf discovered thus far.

2. Observations

Table 1 lists the objects observed and provides a summary of their photometric properties and spectral classification based on the far-optical spectroscopy by Kirkpatrick et al. (1999). As part of the “first light” scientific commissioning of the NIRSPEC spectrograph at the W. M. Keck Observatory on Mauna Kea, Hawaii, near-infrared spectra of this sample were obtained. Kelu-1 (Ruiz et al. , 1997), was observed on April 29, 1999, but all of the other sources were observed on June 2, 1999. Since detailed descriptions of the design and performance of NIRSPEC are given elsewhere, (McLean et al. 1998, McLean et al. 2000), only a short summary is included here. Briefly, this cryogenic instrument is the world’s first facility-class infrared spectrograph employing the state-of-the-art 1024×1024 InSb array. For the highest spectral resolution work, a cross-dispersed echelle grating

is used which yields $R=25000$ for a $0.43''$ wide slit, corresponding to 3-pixels along the dispersion direction. A much lower resolution mode can be obtained simply by replacing the echelle grating with a flat mirror and using the cross-dispersion grating alone. The spectral resolution in this mode is $R \sim 2500$ for a 2-pixel wide slit (corresponding to $0.38''$ in this case).

For the present study, the lower resolution mode was selected for speed and efficiency. The goal was to obtain a spectral sequence of L-dwarfs with good signal-to-noise ratios from about $1\text{--}2.5 \mu\text{m}$. Only the J-band results, covering the interesting range from $1.135 - 1.362 \mu\text{m}$ are discussed in this short note.

As shown in Table 1, the J magnitudes of the sample range from 12.8 to 16.3. All objects received the same total exposure time of 600 seconds. The observing strategy employed was to obtain a 300 s integration at each of two positions along the entrance slit separated by about $20''$, referred to as a nodded pair. Seeing conditions were generally very good for these measurements ($0.3''\text{--}0.5''$) and a slit width of $0.38''$ was used in all cases. To calibrate for absorption due to the Earth's atmosphere, stars of spectral type A0 V to A2 V were observed as close to the same airmass as possible (typically within 0.05 airmasses, except for 2MASSW J1632+1904 for which the difference was 0.28) and also close in time. The J-band is sensitive to atmospheric extinction due mainly to water vapor absorption. A-type stars are essentially featureless in this region except for the Paschen Beta line at $1.2816 \mu\text{m}$, which can be interpolated out. Immediately after the observation of each source, both neon and argon arc lamp spectra were obtained for wavelength calibration, and a white-light spectrum was recorded for flat-fielding.

Reduction of the data followed the steps set out below. The first requirement is to place the raw data on a uniform grid of wavelength and position along the slit. Using custom software developed by one of us (James Larkin) the spatial distortions were corrected first. A spatial map was formed by using the sum of the nodded pair of standard star spectra with the assumption that the pair of spectra must be exactly a fixed number of pixels apart. Next, the arc lamp spectra were used to construct a spectral map to warp the raw data onto a uniform wavelength scale using a second order polynomial fit. Next, the A-type calibration star was reduced by forming the difference image, warping it with the spatial and spectral mapping routines, dividing by the normalized flat field lamp, shifting and co-adding the pair of spectra at the two slit positions and then extracting the resultant spectrum. Division with a blackbody spectrum for the temperature corresponding to the star's published spectral class completed the reduction of the standard star. Finally, the Paschen Beta absorption line at $1.2816 \mu\text{m}$ was removed by interpolation from the reduced spectra before it was used for division into the corresponding object spectra.

Similar steps were applied to the raw data frames of the target sources. After rectification and flat-field correction, each spectrum was extracted and divided by the fully-reduced spectrum of its associated calibration star. Finally, the nodded pair of reduced spectra were shifted, co-added together and extracted to give the resultant calibrated spectrum of each source. The results are shown in Figure 1. Note that this entire set of new infrared spectra for a sample of seven optically-faint, low-mass objects represents a total of only 70 minutes of on-source observing time, comparable to the exposure time *per* object needed with other instruments or at shorter wavelengths.

3. Results

Clearly, the strongest atomic line transitions in this wavelength region are the pair of neutral potassium (K I) lines at 1.1690, 1.1770 μm and 1.2432, 1.2522 μm respectively. The first pair correspond to the multiplet designation 4p $^2\text{P}^o$ - 3d ^2D , and the second pair are from the 4p $^2\text{P}^o$ - 5s ^2S multiplet. The dominant molecular species in the L-dwarfs in this band are H₂O and iron hydride (FeH), with methane (CH₄) appearing in the T-dwarf. The strongest FeH bands are expected at 1.194, 1.21 and 1.237 μm approximately. A pair of sodium lines, the 3p $^2\text{P}^o$ - 4s ^2S multiplet, can just be detected buried in the water absorption at 1.138 and 1.141 μm and we report the detection of a weak rubidium line at 1.3233 μm (5p $^2\text{P}^o$ - 6s ^2S) as well as the cesium line at 1.3588 μm (6p $^2\text{P}^o$ - 7s ^2S) in the spectrum of 2MASSW J1507. Many other features are evident however, and even the smallest spectral structures are real and above the noise level. Distinctive patterns of lines around 1.25-1.33 μm repeat from object to object among the earlier spectral types but fade out in the later spectral classes. Comparison of the region from 1.16–1.22 μm in our L-dwarf spectra with the same region studied in M-dwarfs by Jones et al. 1996 (see their Fig. 2 for Gl 406) using CGS4 on UKIRT, reveals excellent detailed agreement.

Although the spectra are still heavily blended even at $R \sim 2500$, we have extracted equivalent widths and full widths at the base of each line for the four K I transitions. We have also constructed an index to measure the strength of the H₂O absorption using the ratio of the flux at 1.33 μm to that at 1.27 μm . The results are summarized in Table 2. The equivalent width of the K I lines changes very slowly from an average of about 7 \AA across the L-dwarfs to about 12 \AA in the T-dwarf SDSS1624, although the line depth decreases significantly. This behavior is due to line broadening. The full width at the base of these lines increases from about 40 \AA in the L-dwarfs to over 80 \AA in the T-dwarf. The water index slowly strengthens from about 0.6 to 0.4 through the L-dwarfs as the absorption at 1.33 μm becomes deeper and then drops markedly to about 0.04 in the T-dwarf.

4. Discussion

The variation in the J-band spectra of this sample of objects is quite remarkable and it is relatively easy to place the objects in a temperature sequence. The water band strengthens as the temperature decreases. FeH weakens and then disappears, the K I lines weaken and broaden and the continuum around $1.15 \mu\text{m}$ slowly drops relative to the continuum at $1.26 \mu\text{m}$. As expected, the DENIS L5 source and the 2MASS L5 object exhibit almost identical spectral characteristics. By ordering the spectra according to the classifications given by Kirkpatrick et al. (1999, 2000), with the earliest spectral type (L2) at the top, the following trends are apparent in the J-band spectra.

L2 (Kelu-1): strong K I and FeH lines are superimposed on a larger depression across the region, which is perhaps the result of residual oxide (either TiO and/or VO) absorption; VO is expected around $1.19 \mu\text{m}$.

L4 (GD165B): any residual oxide absorption has gone, effectively raising the continuum to produce a flatter spectrum, and making the K I and FeH features appear stronger although they are expected to decrease with decreasing temperature. The water absorption (steam) band at $1.30 \mu\text{m}$ is increasing in strength. Numerous small features from $1.25\text{--}1.30 \mu\text{m}$ closely match those in Kelu-1.

L5 (2MASSW J1507-1627): all features present in the L4 class remain. The K I and FeH features are very slightly weaker, while the water band at 1.30 microns is deeper than before and there is a slight slope of the continuum towards the blue end.

L5 (DENIS-P J1228-1547): this spectrum is almost the same as the previous one, confirming that they are indeed the same spectral class.

L8 (2MASSW J1623+1904): at L8, the FeH features have disappeared and the depth of the K I lines are significantly weaker but there is evidence of broadening in their wings. There is a slight downward slope of the continuum towards the blue. The steam band is relatively stronger.

L8/9 (2MASSW J1523+3014): Very similar to the previous L8, but the K I lines appear slightly broader and the water band is slightly deeper. The slope to the blue is a little stronger than in L8. Consequently, this object may be cooler than 2MASSW J1623+1904 as its designation suggests, but the difference is small.

T (SDSS 1624+0029): A dramatic slope towards the blue appears, due to the onset of methane absorption in this wavelength region, and there is also a slope or “break” towards the red from about $1.26\text{--}1.31 \mu\text{m}$ before a deep water band sets in. The K I lines are still present but are now very broad.

As an illustration of the density of molecular features and the problem of line blending, Figure 2 shows a model spectrum kindly provided by Peter Hauschildt (private communication). This sample spectrum is based on a model atmosphere code (AMES-Dusty,

Allard & Hauschildt. in prep), with a self-consistent treatment for dust formation. The treatment of dust is complicated however, and theorists have yet to agree on the best approach. The parameters of this model are solar metallicity, $\log(g)=4.5$ and $T_{eff}=2000$ K and the model spectrum was smoothed from an original resolution of $R=50,000$. Qualitatively, the agreement with the NIRSPEC spectra is very good.

Another useful framework for understanding these spectra is the molecular equilibrium calculations by Burrows and Sharp (1999). As their analysis shows, the main absorbers characteristic of M stars (*e.g.* TiO and VO) decline rapidly in importance with decreasing effective temperature. These molecules are expected to condense onto dust grains; TiO for instance forms perovskite (CaTiO_3). The abundance of gaseous TiO begins to decrease around 2400 K and similarly, VO will become depleted near 1800 K. For iron, the first condensate to form is the metal itself, at about 2200 K, which can then form droplets and rain out of the atmosphere. We have carefully compared our spectra to the solar atlas and cannot make any conclusive identifications with iron lines, or any other metal lines (such as Mn and Al) among the dense forest of H_2O transitions. Interestingly, Jones et al. 1996 noted the presence of Fe in earlier spectral types, such as the M6 dwarf GL406, at a comparable resolution. A significant amount of iron may have rained out.

Since they are less refractory and survive in monatomic form for a greater temperature range, the neutral alkali metals (Na, K, Rb, Cs) are expected to remain after the true metals become depleted. In effect, as the temperature falls the atmospheres of cool sub-stellar objects become more transparent. The column density of potassium and sodium, for instance, is expected to increase to the point where the wings of the absorption lines become damped. This result explains the strength, broadening and temperature dependence of the K I lines seen in our spectra. According to Burrows and Sharp (1999), sodium and potassium should become depleted around 1500 - 1200 K, with sodium disappearing first and potassium forming into KCl below about 1200 K. If there is settling of refractory species however, at higher, deeper temperatures, then both atomic sodium and potassium are expected to persist to lower temperatures, at which point they should form their sulfides, not chlorides (see Burrows, Marley and Sharp 1999, and Lodders 1999). Figure 1 shows that the very strong K I lines persist, albeit with broad wings, well into the T-dwarf temperature range.

Some features apparent in the new data are not yet explained by the existing models. For example, a broad, relatively strong feature is seen in our spectra at $1.22 \mu\text{m}$. This feature remains through L5, but is gone in the L8 spectra. Although this is the same pattern as followed by FeH, this broad feature does not appear in the opacity plot of FeH kindly supplied by Adam Burrows (private communication), nor in the model spectrum provided

by Peter Hauschildt. Finally, our results imply that any L- or T- dwarf object meeting the discovery parameters of the 2MASS and/or the SDSS can be observed spectroscopically with NIRSPEC on Keck at medium to high spectral resolution. The near-infrared region from 1.13 - 1.36 μm is quite rich in spectral features, most of which appear to be unresolved blends of molecular species, namely H_2O and FeH in the L-dwarfs and CH_4 in the T-dwarfs. Evidently, even higher spectral resolution would help to constrain the models.

It is a pleasure to acknowledge the hard work of past and present members of the NIRSPEC instrument team at UCLA: Maryanne Anglonto, Odvar Bendiksen, George Brims, Leah Buchholz, John Canfield, Kim Chim, Jonah Hare, Fred Lacayanga, Samuel B. Larson, Tim Liu, Nick Magnone, Gunnar Skulason, Michael Spencer, Jason Weiss, Woon Wong. In addition we thank director Fred Chaffee, CARA instrument specialist Thomas A. Bida, and the Observing Assistants at Keck observatory, Joel Aycock, Gary Puniwai, Charles Sorenson, Ron Quick, and Wayne Wack, for their support. We are pleased to acknowledge the International Gemini Telescopes Project for the InSb detector used in these measurements. Finally, we gratefully acknowledge Adam Burrows and Peter Hauschildt for very helpful information and advice about the current model atmospheres of low-mass stars and sub-stellar objects.

REFERENCES

- Allard, F., Hauschildt, P.H., Alexander, D.R. and Starrfield, S. 1997, *Annu. Rev. Astron. Astrophys.*, 35, 137.
- Burrows, A. and Sharp, C.M. 1999, *ApJ*, 512, 843
- Burrows, A., Marley, M.S. & Sharp, C.M. 1999, in press
- Delfosse, X., et al. 1997, *A & A*, 327, L25
- Geballe, T.R., Kulkarni, S.R., Woodward, C.E. and Sloan, G.C. 1996, *ApJ*, 467, L101
- Jones, H.R. A., Longmore, A. J., Allard, F., and Hauschildt, P. H. 1996, *MNRAS*, 280, 77
- Kirkpatrick, J.D., Kelly, D.M., Rieke, G.H., Liebert, J., Allard, F., Wehrse, R. 1993, *ApJ*, 402, 643
- Kirkpatrick, J.D., Reid, I.N., Gizis, J.E., Burgasser, A.J., Liebert, J., Monet, D.G., Dahn, C.C., and Nelson, B. 2000, *ApJ*, in prep.
- Kirkpatrick, J.D., Reid, I.N., Liebert, J., Cutri, R.M., Nelson, B., Beichman, C.A., Dahn, C.C., Monet, D.G., Gizis, J.E., and Skrutskie, M.F. 1999, *ApJ*, 519, 802
- Lodders, K. 1999, *ApJ*, 519, 793

- Martin, E. L., Delfosse X., Basri, G., Goldman, B., Forveille, T., & Zapatero-Osorio, M. R. 1999, *AJ*, 118, 2466
- McLean, I.S., et al. 1998, *SPIE*, 3354, 566
- McLean, I.S., et al. 2000, *PASP*, in preparation
- Ruiz, M.T., Leggett, S.K. & Allard, F. 1997, *ApJ*, 491, L107
- Skrutskie, M. F., et al. 1997, in *The Impact of Large-Scale Near-IR Sky Surveys*, ed. F. Garzon (Dordrecht: Kluwer), 25
- Strauss, M. A., et al. , 1999, *ApJ*, 522, L61
- Tinney, C.G. et al. , 1993, *AJ*, 105, 1045.
- Tinney, C.G., Delfosse, X., and Forveille, T. 1997, *ApJ*, 490, L95.

Table 1. **Observed Objects and Summary of their Photometric /Spectral Properties**

Object	RA(2000)	Dec(2000)	J	H	K _s	Sp. Type	Ref.
DENIS-P J1228.2-1547	12 28 13.9	-15 47 11.7	14.38	13.37	12.81	L5	1
Kelu-1	13 05 40.2	-25 41 06	13.38	12.41	11.81	L2	1
GD165B	14 24 40.0	+09 17 24	15.80	14.78	14.17 ^a	L4	1
2MASSW J1507-1627	15 07 47.7	-16 27 39	12.82	11.89	11.30	L5	2
2MASSW J1523+3014	15 23 22.6	+30 14 56	16.32	15.00	14.24	L8/9	2
2MASSW J1632+1904	16 32 29.4	+19 04 41	15.86	14.59	13.98	L8	1
SDSS 1624+0029	16 24 14.4	+00 29 15.6	15.53	15.57	15.70 ^a	T	3

^aThis is K, not Ks.

1.Kirkpatrick, J.D., Reid, I.N., Liebert, J., Cutri, R.M., Nelson, B., Beichman, C.A., Dahn, C.C., Monet, D.G., Gizis, J.E., and Skrutskie, M.F. 1999, ApJ, 519, 802

2.Kirkpatrick, J.D., et al. , 2000, ApJ, in prep

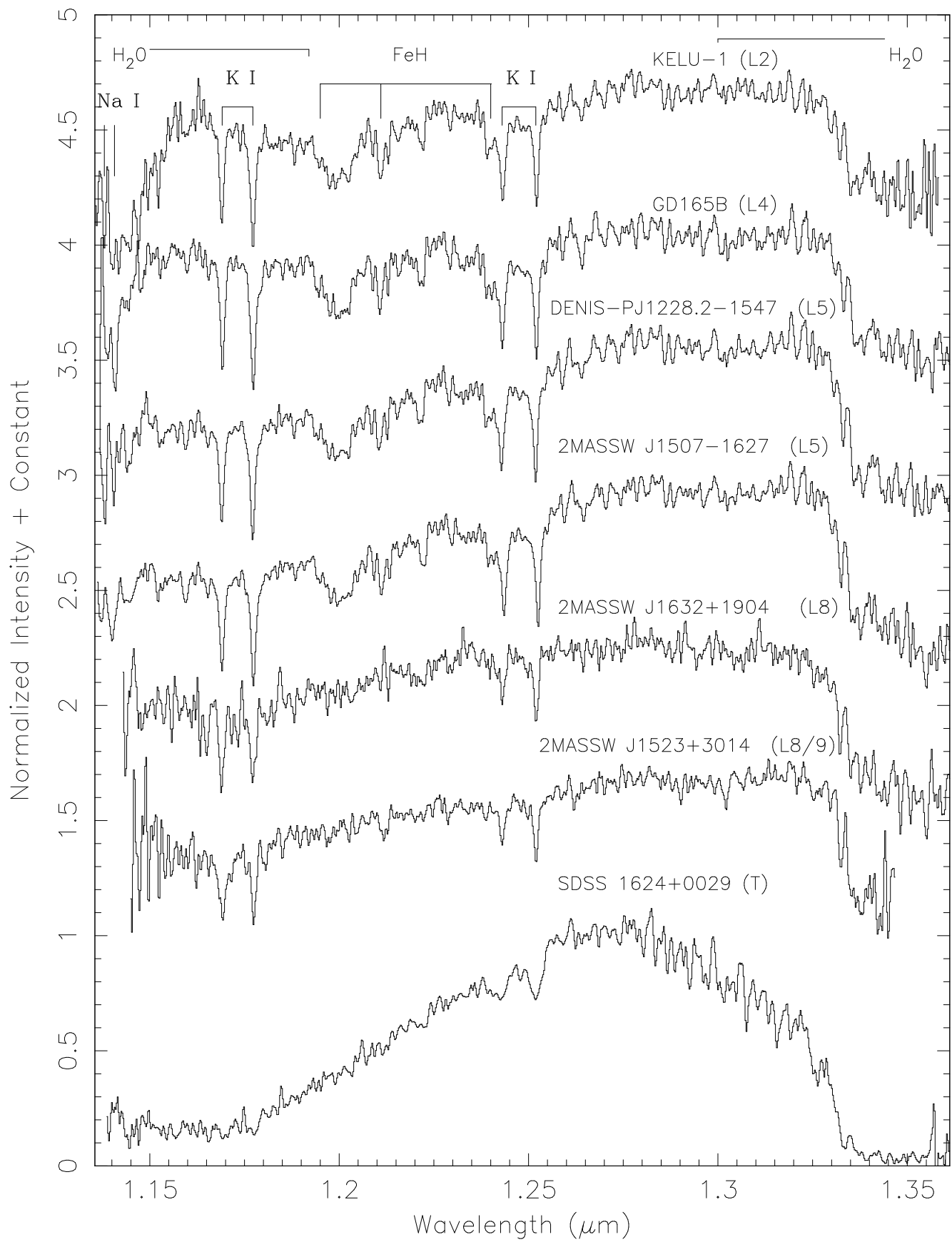
3.Strauss, M. A., et al. , 1999, ApJ, 522, L61

Table 2. **Equivalent Widths (\AA) of the K I lines and the Strength of the H₂O Band at 1.33 μm**

Object	Sp.Type	1.169 μm	1.177 μm	1.244 μm	1.253 μm	1.33 $\mu\text{m}/1.27 \mu\text{m}$
Kelu-1	L2	6.18	6.86	6.64	6.32	0.55
GD165B	L4	6.79	9.34	8.64	7.52	0.56
DENIS-P J1228.2-1547	L5	7.26	9.94	7.88	7.06	0.52
2MASSW J1507-1627	L5	8.98	10.82	7.68	7.84	0.46
2MASSW J1632+1904	L8	7.75	8.35	6.02	7.33	0.38
2MASSW J1523+3014	L8/9	8.83	9.18	6.17	6.56	0.41
SDSS 1624+0029	T	8.93	14.75	9.09	11.38	0.04

Fig. 1.— NIRSPEC spectra with a resolving power of $R=2,500$ (5 \AA) and a dispersion of 2.5 \AA per pixel from 1.135 to 1.357 \mu m for a sample of 6 L-dwarfs and one T-dwarf. Each spectrum has been normalized to unity using the average flux near 1.28 \mu m and then displaced by 0.6 units along the y-axis for clarity of presentation. For the fainter sources, the first few and last few data points are too noisy to plot. Prominent features are identified, but much of the structure is due to blending of molecular transitions.

Fig. 2.— An example of a model spectrum from Hauschildt et al. with a final (smoothed) resolution of $R=2,000$ (6 \AA) from 1.135 to 1.357 \mu m for qualitative comparison with the NIRSPEC data. The model parameters are $\log(g)=4.5$, $T_{eff}=2000 \text{ K}$ and solar metallicity. Lines identified in the model spectrum are not necessarily the same as those seen in the NIRSPEC observations (see text).



Relative Flux

